# Determination of carrier concentration in n-ZnSe by reflectance difference spectroscopy: Experimental results and model calculation



doi: 10.1063/1.1483917

# Determination of carrier concentration in *n*-ZnSe by reflectance difference spectroscopy: Experimental results and model calculation

N. Kumagai,[a] T. Hanada, and T. Yao
*Institute for Materials Research, Tohoku University, 2-1-1 Katahira, Aoba-ku, Sendai 980-8577, Japan*

T. Yasuda
*Joint Research Center of Atom Technology, National Institute for Advanced Interdisciplinary Research, 1-1-4 Higashi, Tsukuba 305-0046, Japan*

(Received 4 June 2001; accepted for publication 16 April 2002)

We have performed *in situ* and *ex situ* measurements of reflectance difference (RD) spectra for Cl-doped *n*-type ZnSe grown by molecular beam epitaxy. The linear electro-optic (LEO) effect (or Pockels effect) in the depletion layer induces characteristic RD features near the $E_1$ and $E_1+\Delta_1$ transition energy. The intensity of these features is correlated with the carrier concentration determined from capacitance–voltage measurements. A quantitative model is presented to explain the observed dependence of the LEO signal on the carrier concentration. This model quantitatively considers the effect of the finite surface state density. A good fit with the experimental results was obtained by assuming the surface state densities of $3.8\times10^{13}$ and $2.6\times10^{13}$ $cm^{-2}$ $eV^{-1}$, respectively, for *in situ* measurement of a Se-terminated surface at 300 °C and for *ex situ* measurement of an oxide-covered surface at room temperature. © *2002 American Institute of Physics.* [DOI: 10.1063/1.1483917]

## I. INTRODUCTION

Fabrication of semiconductor devices such as laser and light emitting diodes requires strict control of doping during crystal growth in order to realize the device performance as designed. If one could measure the carrier concentration *in situ* during the growth process, for example, during molecular beam epitaxy (MBE) or chemical vapor deposition (CVD), real-time control of the dopant concentration, based on feedback, would be possible. Among the possible techniques for such measurement is reflectance difference spectroscopy (RDS), which measures the in-plane optical anisotropy of the sample. Doped semiconductors generally have a surface depletion layer with quite a strong, built-in electric field ($\sim10^7$ to $10^8$ V/m). If this field is along the [001] direction of the zinc-blende crystal, it induces nonzero anisotropy in the dielectric response, between the [110] and $[1\bar{1}0]$ polarization directions, $\Delta\epsilon$. This effect is called the linear electro-optic (LEO), or Pockels effect. The amplitude of $\Delta\epsilon$ can be quantified by measuring the amplitude of reflectance difference (RD) between the two ploarization directions of light.

Previous RDS measurements on doped III–V and II–VI materials [GaAs,[1,2] ZnSe,[3–6] and ZnTe (Ref. 7)] showed that LEO-induced anisotropy can be detected by RDS. Our previous studies using *ex situ* and *in situ* RDS dealt with Cl-doped *n*-ZnSe. The LEO feature was observed near the $E_1$ (4.9 eV) and $E_1+\Delta_1$ (5.1 eV) transition energies of ZnSe.[5,6] The amplitude of this feature was found to be proportional to $(N_d-N_a)^{1/3}$ in the range $N_d-N_a<2\times10^{18}$ $cm^{-3}$, where $N_d$ and $N_a$ are concentrations of donors and acceptors, respectively. In those studies, the carrier concentration, $N_d-N_a$, was determined from the measurement of the capacitance-voltage. Similar power-law dependence was reported for *p*-type ZnSe.[4] However, a simple band-bending model based on the assumption of surface Fermi-level pinning (i.e., infinite density of the surface states) predicts a 1/2-order dependence on $N_d-N_a$, and there has been no successful explanation for the 1/3-order dependence observed.

In this article we first summarize the experimental results for the LEO features measured for *n*-type ZnSe. Additional data for the temperature dependence of this feature is also given. Then, we describe a model which considers the *finite* density of the surface states in addition to the attenuation of light. This model successfully explains the observed dependence of the LEO amplitude on carrier concentration.

## II. EXPERIMENT

The RDS system used in this study is similar to the one developed by Aspnes *et al*[8]. For (001) samples the RD signal is defined as follows:

$$\frac{\Delta\tilde{r}}{\tilde{r}}=\frac{\tilde{r}_{1\bar{1}0}-\tilde{r}_{110}}{(\tilde{r}_{1\bar{1}0}+\tilde{r}_{110})/2}, \tag{1}$$

where $\tilde{r}$ is the complex reflectance and the subscripts indicate the directions of the polarization of light. Both the real and imaginary parts of $\Delta\tilde{r}/\tilde{r}$ were measured. In this article, we only show the spectra for the real parts of $\Delta r/r$.

The samples were prepared by growing ZnSe on undoped GaAs(001) substrates using MBE. The ZnSe layer was typically more than 300 nm thick. It was therefore much thicker than the penetration depth of light in the energy range of our interest (4.0 ~ 5.8 eV). $ZnCl_2$ was used as a Cl source for *n*-type doping. We performed *in situ* RDS measurements

[a]Electonic mail: naoto-kumagai@aist.go.jp

 

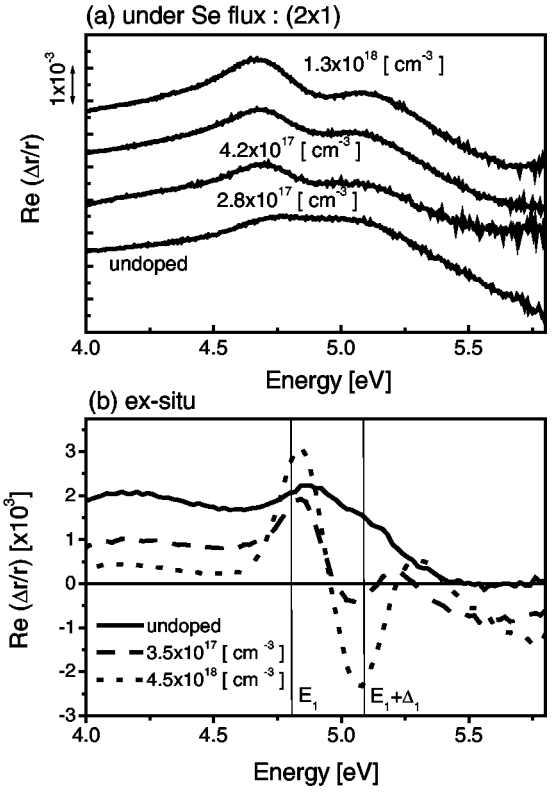


FIG. 1. RD spectra for Cl-doped ZnSe samples with different carrier concentrations: (a) *in situ* measurement under a Se beam (see Ref. 5), and (b) *ex situ* surface (covered with natural oxide layer).

for both the Zn- and Se-terminated surfaces at a growth temperature of 300 °C under each beam. The $ZnCl_2$ beam was blocked during the measurement, although a spectrum taken with the $ZnCl_2$ beam present was essentially the same as that with the $ZnCl_2$ beam blocked. In *in situ* measurements, we focused on the spectral region near the $E_1$ (4.8 eV) and $E_1+\Delta_1$ (5.1 eV) transitions of ZnSe where characteristic LEO features appear due to the resonance effect. LEO signatures around the $E_0$ and $E_0+\Delta_0$ transitions (2.6–3.1 eV) could not be distinguished from the strong interference fringes.

The effect of temperature on the LEO signature was investigated for a sample with $N_d-N_a=1.3\times10^{18}$ cm$^{-3}$. In this experiment, RDS measurement was first carried out at growth temperature. The temperature of the sample was then decreased to 250, 200, and 150 °C, and the RDS spectrum was measured at each temperature. The sample was placed under a Se beam during these measurements. The surface reconstruction observed by RHEED was $(2\times1)$ at 300 and 250 °C, and it changed to $c(2\times2)$ at 200 and 150 °C. The changes in the surface reconstruction were in agreement with those reported by Zettler *et al.*[9]

After the samples were taken out of the MBE chamber, *ex situ* RDS measurements were performed in air at room temperature. In this case, the surface was covered with a natural oxide layer. The carrier concentration for each sample was evaluated using the capacitance-voltage ($C$–$V$) method. The $N_d-N_a$ value of the prepared samples ranged from $2\times10^{17}$ to $8\times10^{18}$ cm$^{-3}$.

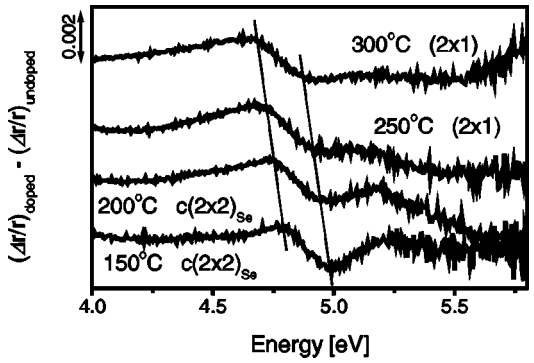


FIG. 2. *In situ* LEO feature for Se termination with decreasing substrate temperature. Reconstructed patterns observed by reflection high-energy electron diffraction are noted for each spectrum. The spectra were obtained by subtracting the spectrum of an undoped sample from that of a doped sample; both were measured at the same temperature.

## III. EXPERIMENTAL RESULTS

Figure 1 shows typical RD spectra measured for ZnSe with different carrier concentrations. *In situ* and *ex situ* results are shown in Figs. 1(a) and 1(b), respectively. $N_d-N_a$ values determined from $C$–$V$ measurement are noted in the figure. In Fig. 1(a), the spectra for the doped samples show positive and negative peaks at 4.7 and 4.9 eV, respectively. With an increase in $ZnCl_2$ cell temperature, and thus an increase in dopant concentration, these peaks become stronger. These features can be ascribed to the LEO effect. Their peak positions also shifted slightly to a lower energy with an increasing doping level. For Zn terminated surfaces, the surface-anisotropy peak due to $c(2\times2)$ reconstruction overlaps the negative LEO peak at 4.9 eV. Therefore it was difficult to distinguish the LEO peak from the surface-anisotropy peak.

The *ex situ* RD spectra in Fig. 1(b) show essentially the same LEO features as in Fig. 1(a). The peaks appear at slightly higher energies in Fig. 1(b) than in Fig. 1(a), because the former were measured at room temperature. The relative positions of the positive and negative peaks with respect to the $E_1$ and $E_1+\Delta_1$ transition energies of ZnSe are similar to those for $n$-type GaAs reported by Tanaka *et al.*[1] For the LEO features of both $n$-GaAs and $n$-ZnSe, the positive peak appears near $E_1$, and the negative one near $E_1+\Delta_1$.

Figure 2 shows the change in the LEO feature with decreasing temperature. Each spectrum in this figure was obtained by subtracting the spectrum of an undoped sample from that of a doped sample; both were measured at the same temperature. This subtraction procedure was necessary because the decrease in substrate temperature causes a change in the surface reconstruction that eventually alters the surface-originated RD signal. After the subtraction, there is little contribution to the spectra from the surface-originated RD, so the effects of temperature on the LEO signature can be clearly seen. As anticipated, the line shape of the LEO signature becomes sharper and larger in amplitude and shifts to a higher energy position with a decrease in substrate temperature.

Figure 3 shows the correlation between the derivative intensity of the *in situ* and *ex situ* LEO signature and the

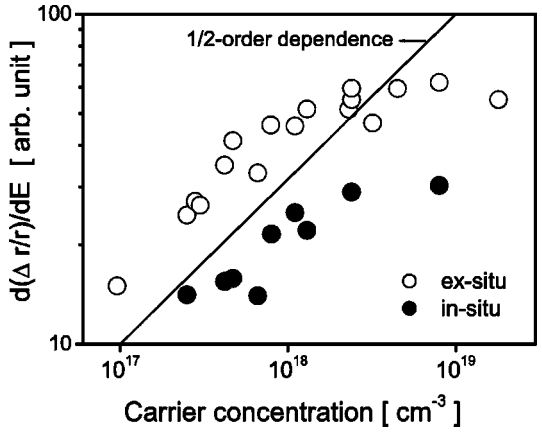


FIG. 3. Correlation between carrier concentration and energy derivation of the LEO signatures. ○: *ex situ* results; ●: *in situ* results.

$N_d - N_a$. The amplitude of the LEO signal was evaluated by calculating the energy derivative of the measured spectrum and then measuring the peak-to-peak height in a similar way as in our previous studies.[5,6] Both the *in situ* and *ex situ* data are shown in this plot. There are more data points for the *ex situ* data set than the *in situ* one because our previous *ex situ* results[5] were also included in this figure. We found that for both *in situ* and *ex situ* data sets, the LEO intensity has a similar dependence on $N_d - N_a$. When $N_d - N_a$ is lower than $10^{18}$ cm$^{-3}$, the LEO amplitude is proportional to $(N_d - N_a)^n$ where $n$ is approximately 1/2. When $N_d - N_a$ is larger than $3\times10^{18}$ cm$^{-3}$, the LEO amplitude nearly saturates for both the *in situ* and *ex situ* results.

The apparent LEO amplitude is smaller for the *in situ* measurement than for the *ex situ* measurement because of the temperature-induced broadening effect shown in Fig. 2.

The technological significance of the correlation shown in Fig. 3 is that $N_d - N_a$ can be directly estimated during growth by measuring the LEO amplitude *in situ*. If the estimated $N_d - N_a$ value is out of the target range, doping control in real time, based on feedback, can be done by adjusting the $ZnCl_2$ source temperature to obtain the desired doping level.

## IV. MODEL DESCRIPTION

As mentioned in the Introduction, a simple band-bending model with the attenuation of light could not explain the saturation of the LEO feature at high carrier concentrations. In this section we describe an improved model for the calculation of the average electric field in the depletion layer. This model considers the finite density of the surface state, as opposed to the previously assumed surface Fermi-level pinning.

The optical anisotropy induced by the LEO effect is linearly proportional to the strength of the electric field, $F$. When $F$ is in the [001] direction, the difference in the complex dielectric function between the [110] and $[1\bar{1}0]$ polarizations, $\Delta\tilde{\epsilon}$, is expressed as

$$\Delta\tilde{\epsilon} = \tilde{\epsilon}_{1\bar{1}0} - \tilde{\epsilon}_{110} = 2\tilde{r}_{41}(\tilde{n}_0)^4 F, \tag{2}$$

where $\tilde{r}_{41}$ is the nonzero component in the LEO tensor (third-rank and complex) for a cubic zinc-blende structure,[10] and $\tilde{n}_0$ is the refractive index at zero field. In the case of a uniformly doped sample, the electric field in the surface depletion layer has a linear profile as a function of depth, $z$:

$$F(z) = \frac{q(N_d - N_a)W}{\epsilon_0 \epsilon_s}\left(1 - \frac{z}{W}\right), \tag{3}$$

where $W$ is the width of the depletion layer, $q$ is the elementary charge, $\epsilon_0$ is the dielectric constant of vacuum, and $\epsilon_s$ is the lowest limitation of frequency for ZnSe.

An average of the $\Delta\tilde{\epsilon} = \langle\Delta\tilde{\epsilon}\rangle$ is calculated using the equation derived by Frova and Aspnes,[11]

$$\langle\Delta\tilde{\epsilon}\rangle = -2iK\int_0^W \exp(2iKz)\Delta\tilde{\epsilon}(z)\,dz, \tag{4}$$

where $K$ is the propagation constant, defined as $2\pi\tilde{n}/\lambda$. This averaging takes into account the attenuation of light.

By substituting Eqs. (2) and (3) into Eq. (4) we obtain

$$\langle\Delta\tilde{\epsilon}\rangle = 2\tilde{r}_{41}\tilde{n}_0^4\langle F\rangle \tag{5}$$

and

$$\langle F\rangle = -2iK\int_0^W \exp(2iKz)\left(1 - \frac{z}{W}\right)dz\frac{q(N_d - N_a)W}{\epsilon_0\epsilon_s}. \tag{6}$$

$\langle F\rangle$ represents the average of $F(z)$ in the depletion layer. The RD signal of the LEO effect is expressed using $\langle\Delta\tilde{\epsilon}\rangle$ as follows:

$$\left.\frac{\Delta\tilde{r}}{\tilde{r}}\right|_{\mathrm{LEO}} = \frac{\langle\Delta\tilde{\epsilon}\rangle}{\tilde{n}_0(\tilde{\epsilon}-1)}. \tag{7}$$

Calculation of the LEO line shape by Eq. (7) requires the spectral data for $\tilde{r}_{41}$, which is not available at present. For the purpose of interpreting the data in Fig. 3, we instead calculated the $\langle F\rangle$ average electric field, which is proportional to the amplitude of the LEO signature.

$$\langle F\rangle = \frac{q(N_d - N_a)W}{\epsilon_0\epsilon_s}\int_0^W\left(1 - \frac{z}{W}\right)\exp\left(-\frac{z}{p}\right)dz \Big/ \int_0^\infty \exp\left(-\frac{z}{p}\right)dz \tag{8}$$

$$= \frac{q(N_d - N_a)W}{\epsilon_0\epsilon_s}\left[1 + \frac{p}{W}\left\{\exp\left(-\frac{W}{p}\right) - 1\right\}\right], \tag{9}$$

where $p$ is the penetrating depth (10 nm at 5 eV for ZnSe). Here, the propagation constant $K$ is replaced with $i/p$.

Now, we assume that the surface state density $\delta$ is finite and that the distribution is uniform above the surface neutral level. The surface neutral level is the highest occupied surface state without a charge transfer from the depletion layer, as shown in Fig. 4. Then, surface band-bending is governed by the following contribution,

$$\phi - \frac{(N_d - N_a)W}{\delta} = V_i + E_{fb}, \tag{10}$$

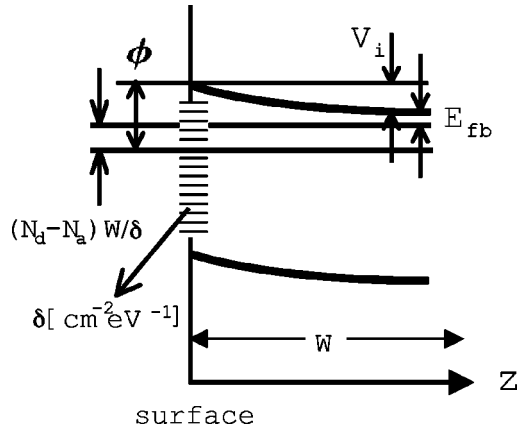


FIG. 4. Schematic diagram of band bending with finite surface density. $\phi$ is the depth of the surface neutral level from the conduction band minimum (CBM) at the surface, $E_{fb}$ is the depth of the bulk Fermi level from the CBM in bulk, and $V_i$ is the built-in potential. If $\delta$ is infinity large, the Fermi level is pinned completely.

where $\phi$ is the depth of the surface neutral level from the conduction band minimum (CBM) at the surface, and $E_{fb}$ is the depth of the bulk Fermi level from the CBM in bulk. The built-in potential $V_i$ is given by

$$V_i = \frac{q(N_d - N_a)}{\epsilon_0 \epsilon_s} W^2. \tag{11}$$

Solving Eqs. (10) and (11) for $W$, we obtain

$$W = \left[ \frac{2\epsilon_0 \epsilon_s (\phi - E_{fb})}{q(N_d - N_a)} + \frac{(\epsilon_0 \epsilon_s)^2}{q^2 \delta^2} \right]^{1/2} - \frac{\epsilon_0 \epsilon_s}{q\delta}. \tag{12}$$

Substituting Eq. (10) into Eq. (9) gives $\langle F \rangle$ with a finite surface state density. When $\delta$ is infinity large and $p/W \ll 1$, $\langle F \rangle$ is proportional to $(N_d - N_a)^{1/2}$. Contrarily, if $\delta$ is finite or $p/W$ is sufficiently larger than unity, $\langle F \rangle$ should deviate from the 1/2 order dependence.

## V. RESULTS AND DISCUSSION

In this section we use the above-mentioned model to calculate the dependence of $\langle F \rangle$ on carrier concentration.

Using Eqs. (9) and (12) we can calculate $\langle F \rangle$ if $\phi - E_{fb}$ and $\delta$ are given. We assume $\phi - E_{fb}$ to be half of the band gap energy. The calculated $\langle F \rangle$ for $\delta = 1 \times 10^{12}$, $1 \times 10^{13}$, and $1 \times 10^{14}$ cm$^{-2}$ eV$^{-1}$ are shown in Fig. 5(a). The dielectric constant at room temperature was used for this calculation. For $\delta = 10^{12}$ cm$^{-2}$ eV$^{-1}$, the deviation from the 1/2 order dependence is clear for the $N_d - N_a$ range of $10^{16}$–$10^{18}$ cm$^{-3}$. For $\delta = 10^{13}$ and $10^{14}$ cm$^{-2}$ eV$^{-1}$, $\langle F \rangle$ is proportional to $(N_d - N_a)^{1/2}$ for $N_d - N_a < 10^{18}$ cm$^{-3}$. In either case, $\langle F \rangle$ shows clear saturation and fall-off as $N_d - N_a$ is increased to $> 10^{18}$ cm$^{-3}$. These results indicate that $\langle F \rangle$, which is approximately proportional to the amplitude of the LEO signal, is affected strongly by the surface state density.

The fall-off predicted for high $N_d - N_a$ and low $\delta$ is due to both a decrease in $V_i$ and a decrease in $W$ below the penetration depth of light.

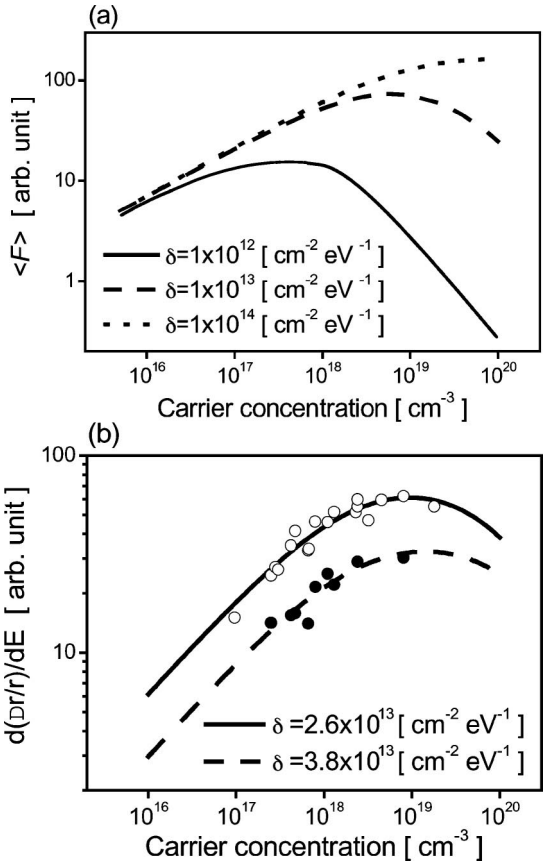


FIG. 5. (a) Calculated results of average electric field, $\langle F \rangle$. (b) Fitting to the experimental results in Fig. 3.

As mentioned above, the amplitude of the LEO signal is supposed to be proportional to $\langle F \rangle$. In Fig. 5(b) we show the result of fitting to the data in Fig. 3. In this fitting, $\langle F \rangle$-$(N_d - N_a)$ curves, as in Fig. 5(a), were calculated using a variable parameter of $\delta$. These curves were then scaled to fit the data in Fig. 3. The best fit was obtained with $\delta = 3.8 \times 10^{13}$ and $2.6 \times 10^{13}$ cm$^{-2}$ eV$^{-1}$ for the *in situ* and *ex situ* results, respectively.

The values obtained for surface state density in our calculated results compare well with those reported in other studies of the surface state density of naturally oxidized semiconductors. Spicer *et al.* reported that the semiconductor-oxide surface state density of $\sim 10^{13}$ cm$^{-2}$ eV$^{-1}$ was around the midgap of an as-grown GaAs(110).[12] Hasegawa *et al.* also reported a similar value for the surface state density of an as-grown (anodic oxidation) GaAs(100).[13] Additionally, Yamagata *et al.* reported that the interface state density at a homointerface between *n*-ZnSe and air-exposed *n*-ZnSe grown by MBE was $\sim 10^{12}$ cm$^{-2}$ eV$^{-1}$ at the midgap.[14]

## VI. CONCLUSION

We performed *in situ* RDS measurements of the LEO signatures of Cl-doped n-type ZnSe during MBE growth. *Ex situ* measurements were also performed after growth. We found that the observed dependence of the LEO feature on $N_d - N_a$ is well explained by a model that considers finite

surface state density. Surface Fermi-level pinning is not always an adequate assumption for the interpretation of the LEO signature.

A fully quantitative analysis of the LEO signature requires the spectroscopic data for $\tilde{r}_{41}$. Efforts are under way to obtain the data by measuring the LEO signal under an externally applied dc field.

## ACKNOWLEDGMENTS

This study was supported in part by a Grant-in-Aid from the Ministry of Science, Culture, Sports and Education (Japan Society for the Promotion of Science) and the Visiting Researcher's Program of the Institute for Materials Research, Tohoku University.

[1] H. Tanaka, E. Colas, I. Kamiya, D. E. Aspnes, and R. Bhat, Appl. Phys. Lett. **59**, 3443 (1991).
[2] Y. H. Chen, Z. Yang, R. G. Li, and Y. Q. Wang, Phys. Rev. B **55**, 7379 (1997).
[3] H. H. Farrell, M. C. Tamargo, T. J. Gmitter, A. L. Weaver, and D. E. Aspnes, J. Appl. Phys. **70**, 1033 (1991).
[4] C. G. Jin, T. Yasuda, K. Kimura, A. Ohtake, L. H. Kuo, T. H. Wang, S. Miwa, T. Yao, and K. Tanaka, Jpn. J. Appl. Phys., Part 1 **36**, 6638 (1997).
[5] N. Kumagai, H. D. Jung, T. Hanada, Z. Zhu, T. Yasuda, K. Kimura, S. D. Lee, M. H. Jeon, H. S. Park, T. I. Kim, and T. Yao, J. Cryst. Growth **184–185**, 505 (1998).
[6] N. Kumagai, T. Yasuda, T. Hanada, and T. Yao, J. Cryst. Growth **214–215**, 547 (2000).
[7] D. Stifter, M. Schmid, K. Hingerl, A. Bonanni, M. Garcia-Rocha, and H. Sitter, Appl. Phys. Lett. **73**, 3857 (1998).
[8] D. E. Aspnes, J. P. Harbison, A. A. Stunda, L. T. Florez, J. Vac. Sci. Technol. A **6**, 1327 (1988).
[9] J. T. Zettler, K. Stahrenberg, W. Richter, H. Wenisch, B. Jobst, and D. Homel, J. Vac. Sci. Technol. B **14**, 2757 (1996).
[10] A. Yariv, *Optical Electronics*, 4th ed. (Saunders, Philadelphia, 1991), p. 314.
[11] D. E. Aspnes and A. Frova, Solid State Commun. **7**, 155 (1969).
[12] W. E. Spicer, P. W. Chye, P. R. Skeath, C. Y. Su, and I. Lindau, J. Vac. Sci. Technol. **16**, 1422 (1979).
[13] H. Hasegawa, L. He, H. Ohno, T. Sawada, T. Haga, Y. Abe, and H. Takahashi, J. Vac. Sci. Technol. B **5**, 1097 (1987).
[14] Y. Yamagata, T. Sawada, K. Imai, and K. Suzuki, J. Cryst. Growth **201/202**, 623 (1999).